



## Predictions of nuclear charge radii and physical interpretations based on the naive Bayesian probability classifier

Yunfei Ma <sup>1</sup>, Chen Su,<sup>1</sup> Jian Liu,<sup>1,2,\*</sup> Zhongzhou Ren,<sup>3</sup> Chang Xu,<sup>4</sup> and Yonghao Gao <sup>1</sup>

<sup>1</sup>College of Science, China University of Petroleum (East China), Qingdao 266580, China

<sup>2</sup>National Superconducting Cyclotron Laboratory and Department of Physics and Astronomy, Michigan State University, East Lansing, Michigan 48824, USA

<sup>3</sup>School of Physics Science and Engineering, Tongji University, Shanghai 200092, China

<sup>4</sup>Department of Physics, Nanjing University, Nanjing 210093, China



(Received 2 August 2019; revised manuscript received 20 November 2019; published 6 January 2020)

**Background:** The nuclear charge radii provide direct information for the nuclear structures. In recent years, many pioneering researches have been devoted to the nuclear charge radii based on the Bayesian neural networks (BNN) method.

**Purpose:** The neural networks always have complex structure. To analyze the data relationships clearly, a statistical method is introduced to study the nuclear properties by combining the sophisticated nuclear models with the naive Bayesian probability (NBP) classifier.

**Method:** In the framework of the NBP method, the predicted charge radii are interpreted as the most reasonable expectations. The prior probabilities and the condition probabilities are computed by the experimental data and the raw results of nuclear models. The posterior probabilities of expectations are updated by the Bayesian formula. The predicted charge radii are regarded as the expectations with maximum probability. Moreover, the abilities of global optimizations and extrapolations of the NBP method are analyzed to demonstrate the availability of the NBP method.

**Results:** For the HFB model and the semiempirical formula, the accuracy of charge radii predictions improves 41% and 32% after NBP refinements, respectively. Calculations also illustrate that the NBP method has robust extrapolating abilities, and the charge radii of unknown regions in the nuclear chart can be predicted by the NBP method.

**Conclusions:** The NBP method contains the advantages of local relations and global descriptions, which can provide fine-tuning for the theoretical results of sophisticated nuclear models. The method proposed in this paper can also be used for other research of nuclear properties.

DOI: [10.1103/PhysRevC.101.014304](https://doi.org/10.1103/PhysRevC.101.014304)

### I. INTRODUCTION

Nuclear charge radii  $R_C$  is an essential quantity for the nuclear property studies, which can reflect the charge density distributions and the Coulomb potentials in nuclei [1,2]. The accurately nuclear charge radii are significant prerequisites in many theoretical studies [3–7]; they can also serve as useful guides for many different experiments, such as electron scattering,  $\alpha$  decay, and nuclear reactions [8–10]. There are a large number of experimental methods to measure the nuclear charge radii, for instance, muonic atom x rays ( $\mu^-$ ) [11], laser spectroscopy [12], optical isotope shifts (OIS) [13],  $K_\alpha$  x-ray isotope shifts ( $K_\alpha$ IS) [14], and high energy elastic electron scattering ( $e^-$ ) [15]. By these methods, more and more charge radii for the nuclei far from the  $\beta$ -stability line are provided [16].

With the experimental developments, many theoretical works have also been processed to investigate the changing

rules of charge radii. There are mainly three ways to describe the  $R_C$ . The first is the Garvey-Kelson (GK) relations [17–19]. The charge radii of the unknown nuclei can be predicted according to its five neighbors. However, the GK relations are only a local effective method, and their extrapolating ability is poor [20,21]. The second is the semiempirical formulas from the “liquid-drop” model (LDM) [22,23]. From the LDM model, we can obtain the relations between the nuclear charge radii  $R_C$  and mass number  $A$ :  $R_C(A) = r_0 A^{1/3}$ . By further introducing the influences of isospin, shell effects, and odd-even staggering, these formulas are further developed in Refs. [13,24,25]. These developed formulas work well in global descriptions of charge radii. However, the semiempirical formulas always have many fitting parameters, and cannot reveal the inner nuclear interactions. The third is the microscopic nuclear structure models, which are mainly constructed from the nuclear effective interactions, and can give microscopic physical descriptions on nuclear inner structure and nucleon configurations [26–28]. As representatives of this method, the Skyrme-Hartree-Fock-Bogoliubov model and the relativistic-mean-field model can well describe the nuclear properties

\*liujian@upc.edu.cn

in nuclear chart both from the  $\beta$ -stability line to the drip-line [29–32]. However, the root-mean-square (RMS) radii deviations from the microscopic nuclear structure models are a little larger, compared with other methods.

In the last few years, the Bayesian neural network (BNN) method is proposed to study the nuclear properties [33–40]. Based on the BNN method, Piekarewicz and Nazarewicz *et al.* obtained significant improvements on predictions of nuclear mass [33], nuclear charge radii [34], and the drip-line locations [35,36]. The artificial neural networks have an amount of advantages in predictions of charge radii. For example, the artificial neural networks are proved to be “the universal approximators,” which could achieve certain desired accuracy for any measurable function [41]. In addition, they can be constructed by multiple different training algorithms, and the fault tolerance abilities are impressive because of the distributed memory [42]. In addition to the studies of nuclear charge radii and nuclear mass, the BNN method was widely applied to other aspects of nuclear physics, such as the jet energy loss distributions in heavy-ion collisions [38], the nuclear  $\beta$ -decay half-lives [39], the two-photon exchange effects [43], and the proton radii [44]. Though without proper supervision there are problems of the under-fitting and over-fitting for the neural networks, many techniques have been developed to solve these problems [45]. However, the artificial neural networks always have complicated structures, which makes it difficult to analyze the data structure and the inner numerical relationship. To overcome these insufficiencies, a developed method is introduced in this paper to study the nuclear properties by combining the nuclear structure models with the naive Bayesian probability (NBP) classifier. The NBP method takes no unknown nodes or layers, which makes the physical analysis of results brief and intuitive. In addition, there are no parameters in the frameworks of the NBP method; therefore, the problems of under-fitting and over-fitting are also avoided.

In this paper, we construct the frameworks of the naive Bayesian probability classifier, and systematically predict the nuclear charge radii by the NBP method. The NBP method implements the refinement of the theoretical models by turning it into a “classification” problem. Primarily, the raw residuals  $\delta(Z, N)$  of charge radii are provided for each nucleus. Then, these values are classified into different classification intervals with a certain classification table, and calibrated as the corresponding classification values  $\delta_i$ . For the candidate nuclei, the probabilities  $P(\delta_i | Z, N)$  of different classification values  $\delta_i$  are calculated by the NBP formula. The classification value  $\delta_i$  with the maximum probability  $P(\delta_i | Z, N)$  is chosen as the estimated residual. Combining the raw results of theoretical models and the predicted residuals of the NBP method, the charge radii of target nuclei can be refined. Both the global and local relations on the properties of different nuclei are taken into account in the framework of the NBP method. Therefore, compared with other local approaches, it can be used to extrapolate to the unexplored regions of the nuclear chart. For the global methods such as the nuclear structure model and liquid-drip model, the applications of the NBP method can also offer minor modifications on the final results by including the necessary nuclear local relationships.

With the NBP method, the theoretical charge radii from the HFB model and Sheng’s semiempirical formula calculations are refined for nuclei in the 2013 charge radii compilation [16]. To analyze the extrapolating abilities of the NBP method, The nuclear charge radii newly added in the 2013 compilation are predicted where the data in the 2004 charge radii compilation [14] are chosen as the learning set. In addition, the refined  $R_C$  of Ca and Bi isotopes are presented to show the predicting abilities of the NBP method for the odd-even staggering. The results show the robust description abilities of the NBP method for the global optimizations and extrapolations. Therefore, the NBP method can be regarded as a general method to predict the nuclear charge radii. The studies in this paper can also be applied to the researches of nuclear mass, nuclear decay, and nuclear reactions.

This paper is organized in four parts: In Sec. II, the theoretical frameworks of the HFB model and the NBP classifier are presented. In Sec. III, the numerical results and discussions are provided. Finally, in Sec. IV, a summary is given.

## II. THEORETICAL FRAMEWORK

In this section, we construct the frameworks of the naive Bayesian probability classifier, and present its formalism to study the nuclear charge radii. The frameworks of the Skyrme-Hartree-Fock-Bogoliubov model are also given, which is used to calculate the raw residuals of charge radii.

### A. The Skyrme-Hartree-Fock-Bogoliubov model

The Skyrme interaction was first proposed by T. H. R. Skyrme in the late 1950s [46]. Further developed by Vautherin, Brink *et al.* in the 1970s, the nuclear Hamiltonian can be written as

$$\begin{aligned}
 H_{\text{Skyrme}}(\mathbf{r}) = & \frac{1}{2} \left[ \left( 1 + \frac{x_0}{2} \right) \rho^2 - \left( x_0 + \frac{1}{2} \right) \sum_q \rho_q^2 \right] \\
 & + \frac{t_1}{4} \left\{ \left( 1 + \frac{x_1}{2} \right) \left[ \rho \tau + \frac{3}{4} (\nabla \rho)^2 \right] \right. \\
 & \left. - \left( x_1 + \frac{1}{2} \right) \sum_q \left[ \rho_q \tau_q + \frac{3}{4} (\nabla \rho_q)^2 \right] \right\} \\
 & + \frac{t_2}{4} \left\{ \left( 1 + \frac{x_2}{2} \right) \left[ \rho \tau - \frac{1}{4} (\nabla \rho)^2 \right] \right. \\
 & \left. + \left( x_2 + \frac{1}{2} \right) \sum_q \left[ \rho_q \tau_q - \frac{1}{4} (\nabla \rho_q)^2 \right] \right\} \\
 & - \frac{1}{16} (t_1 x_1 + t_2 x_2) J^2 + \frac{1}{16} (t_1 - t_2) \sum_q J_q^2 \\
 & + \frac{1}{12} t_3 \rho^\gamma \left[ \left( 1 + \frac{x_3}{2} \right) \rho^2 - \left( x_3 + \frac{1}{2} \right) \sum_q \rho_q^2 \right] \\
 & + \frac{1}{2} W_0 \left( J \nabla \rho + \sum_q \nabla \rho_q \right). \tag{1}
 \end{aligned}$$

In this equation,  $\rho$ ,  $\tau$ ,  $J$  are the nuclear charge density, the kinetic energy density, and the spin density, respectively. With the Hamiltonian in Eq. (1), the Schrodinger equations can be deduced and expressed as

$$\left[ -\nabla \frac{\hbar^2}{2m^*(r)} \nabla + U(\mathbf{r}) + U_{\text{Coul}}(\mathbf{r}) + \frac{1}{i} W(\mathbf{r})(\nabla \times \sigma) \right] \varphi_i(\mathbf{r}) = \epsilon_i \varphi_i(\mathbf{r}), \quad (2)$$

where  $m^*(\mathbf{r})$ ,  $U(\mathbf{r})$ , and  $W(\mathbf{r})$  are the effective nuclear mass, the Skyrme potential, the Coulomb potential, and the spin-orbit potential, respectively [47]. By solving the Schrodinger equations Eq. (2) iteratively, the single-particle wave functions  $\varphi_i$  can be obtained. The nuclear proton densities is

$$\rho_p(r) = \sum_i \varphi_i(\epsilon_i, r)^2. \quad (3)$$

Folding the charge distributions of single proton  $\rho^p(r)$ , we can obtain the nuclear charge density [48]:

$$\rho_c(\mathbf{r}) = \int \rho_p(\mathbf{r}') \rho^p(|\mathbf{r} - \mathbf{r}'|) d\mathbf{r}'. \quad (4)$$

With the charge distributions, the nuclear charge radii can be calculated by

$$R_C = \left[ \int_0^\infty r^2 \rho_c(\mathbf{r}) dr \right]^{1/2}. \quad (5)$$

### B. The naive Bayesian probability method

The NBP classifier, rooted in Bayesian theorem, is usually used to describe the relationship on the conditional probabilities of random events  $A$  and  $B$ . Based on the Bayesian theorem, the conditional probability can be decomposed as [49]

$$P(A_i|B) = \frac{P(B|A_i)P(A_i)}{\sum_{i=1}^n P(B|A_i)P(A_i)}, \quad (6)$$

where the prior probabilities  $P(A_i)$  are not affected by the events  $B$ , and the conditional probabilities  $P(A_i|B)$  represent the chance that events  $A$  happened under the assumption of events  $B$ .

In this paper, the NBP classifier is used to refine the residuals of nuclear charge radii. The residuals represent the deviations between the theoretical results and experimental data. Based on the numerical order of values, the raw residuals  $\delta(Z, N)$  are classed into several observation intervals. For each interval, a classification value  $\delta_i$  is provided, and the residuals  $\delta(Z, N)$  in each interval are calibrated as corresponding classification values  $\delta_i$ . In Table I, we present an example for the classification table, in which the residuals are divided into 10 intervals.

Based on the classification table in Table I, the residuals  $\delta(Z, N)$  for certain nuclei with proton number  $Z$  and neutron number  $N$  can be predicted by the NBP method. The probabilities of 10 classification values  $\delta_i$  in Table I can be calculated by Eq. (6). The events  $A_i$  in Eq. (6) are defined as the classification values  $\delta_i$ . The events  $B$  in Eq. (6) are defined as the proton number  $Z$  and the neutron number  $N$ . Assuming

TABLE I. An example of the classification table with 10 intervals and corresponding classification values. For nuclei whose raw residuals  $\delta(Z, N) = R_{\text{th}} - R_{\text{exp}}$  are in the intervals, the residuals are calibrated as the corresponding classification values  $\delta_i$ .

Intervals (fm)	$\delta_i$ (fm)
$(-\infty, -0.04)$	$\delta_1 = -0.070$
$(-0.04, -0.03)$	$\delta_2 = -0.035$
$(-0.03, -0.02)$	$\delta_3 = -0.025$
$(-0.02, -0.01)$	$\delta_4 = -0.015$
$(-0.01, 0.00)$	$\delta_5 = -0.005$
$(0.00, 0.01)$	$\delta_6 = 0.005$
$(0.01, 0.02)$	$\delta_7 = 0.015$
$(0.02, 0.03)$	$\delta_8 = 0.025$
$(0.03, 0.04)$	$\delta_9 = 0.035$
$(0.04, +\infty)$	$\delta_{10} = 0.070$

that the events are independent of others, the naive Bayesian probability formula can be rewritten as

$$P(\delta_i|Z, N) = \frac{P(\delta_i)P(Z|\delta_i)P(N|\delta_i)}{P(Z)P(N)}. \quad (7)$$

The prior probabilities  $P(\delta_i)$  are the occurrence frequency of classification values  $\delta_i$ .  $P(Z)$  and  $P(N)$  are the occurrence frequency of features  $Z$  and  $N$  in the sample set, respectively. The conditional probabilities  $P(Z|\delta_i)$  and  $P(N|\delta_i)$  represent the occurrence frequency of features  $Z$  and  $N$  in the intervals with the classification values  $\delta_i$ . By comparing the posterior probabilities  $P(\delta_i|Z, N)$  of 10 classification values  $\delta_i$ , the predicted residual for the nucleus  $(Z, N)$  is regarded as the expectation with maximum probability.

The HFB model is chosen as an example to illustrate the applications of the NBP method. There are 896 nuclei with the mass number  $A > 3$  in the 2013 compilation [16], whose experimental data are known. These theoretical nuclear charge radii are calculated by the HFB model, and the raw residuals  $\delta(Z, N)$  of these nuclei can be obtained. We refine the theoretical  $R_C$  of  $^{104}\text{Mo}$  to show the calculation processes of the NBP classifier. The experimental  $R_C$  of  $^{104}\text{Mo}$  is 4.525 fm, and the theoretical result from the HFB model is 4.446 fm. The raw residual  $\delta(Z, N)$  is  $-0.079$  fm. All the nuclei in the 2013 compilation except  $^{104}\text{Mo}$  are chosen as the sample set. According to the raw residuals  $\delta(Z, N)$ , the nuclei in the sample set are classed into 10 intervals in Table I. The residuals of the charge radii in these intervals are calibrated as corresponding classification values  $\delta_i$ . With these data in the sample set, the prior probabilities  $P(\delta_i)$ ,  $P(Z = 42)$ ,  $P(N = 62)$ , and the conditional probabilities  $P(Z = 42|\delta_i)$ ,  $P(N = 62|\delta_i)$  are presented in Table II. The posterior probabilities  $P(\delta_i|Z = 42, N = 62)$  of 10 classification values  $\delta_i$  are calculated by Eq. (7), and the results are also shown in Table II.

In Table II, one can see the classification value  $\delta_1 = -0.070$  fm has the maximum posterior probability  $P(-0.070 \text{ fm}|42, 62) = 0.844$  in 10 different classification values  $\delta_i$ .

TABLE II. The posterior probabilities  $P(\delta_i|Z = 42, N = 62)$  for 10 different classification values  $\delta_i$  of  $^{104}\text{Mo}$  based on the Table I. The 895 nuclei with the mass number  $A > 3$  in the 2013 compilation [16] except itself are chosen as the sample set. The prior probabilities  $P(\delta_i)$ ,  $P(Z = 42)$ ,  $P(N = 62)$  and the corresponding conditional probabilities  $P(Z = 42|\delta_i)$ ,  $P(N = 62|\delta_i)$  are also provided in this table.

$\delta_i(\text{fm})$	$P(\delta_i)$	$P(Z = 42)$	$P(N = 62)$	$P(Z = 42 \delta_i)$	$P(N = 62 \delta_i)$	$P(\delta_i Z = 42, N = 62)$
-0.070	0.203	0.016	0.011	0.032	0.023	0.844
-0.035	0.078	0.016	0.011	0	0.029	0
-0.025	0.099	0.016	0.011	0.011	0.011	0.072
-0.015	0.100	0.016	0.011	0.022	0.011	0.142
-0.005	0.126	0.016	0.011	0	0.009	0
0.005	0.141	0.016	0.011	0.024	0.008	0.152
0.015	0.115	0.016	0.011	0.010	0	0
0.025	0.073	0.016	0.011	0.015	0	0
0.035	0.035	0.016	0.011	0	0	0
0.070	0.035	0.016	0.011	0	0	0

Therefore, we choose  $\delta_1 = -0.070$  fm as its predicted residual. For  $^{104}\text{Mo}$ , the true residual  $\delta(Z, N)$  is  $-0.079$  fm, which has a large difference from the experimental data. The predicted residual from the NBP method is very close to the true residual. The refined  $R_C$  is 4.516 fm for the HFB model. Comparing with the raw result of the HFB model, the accuracy of charge radii predictions improves 89%.

The results of Table II are obtained based on the classification intervals in Table I. In addition to Table I, other classification tables can also be used to refine the charge radii. During the calculations, we used 100 different classification tables with different intervals for the predictions. The final NBP predicted  $\langle R_C \rangle$  for the target nuclei are the average of all the estimates that are generated from different classification tables. The statistical uncertainty can also be quantified for the predictions,

$$\Delta R_C = \sqrt{\langle R_C^2 \rangle - \langle R_C \rangle^2}, \quad (8)$$

where  $\langle R_C^2 \rangle$  is evaluated following the same procedure described before.

### III. RESULTS

With the naive Bayesian probability method described in Sec. II, the nuclear charge radii calculated by the microscopic nuclear structure model and the semiempirical formula are refined in this section. One hundred classification tables are chosen for the predictions. We first discuss the properties of global optimizations for the NBP method, where 896 nuclei with mass number  $A > 3$  in the 2013 compilation [16] are chosen as the entire set. Next, the extrapolating abilities of the NBP method are analyzed. In the last, the refined charge radii of Ca and Bi isotopes are presented to show the predicting abilities of the NBP method for the odd-even staggering.

#### A. Global optimization of the NBP method

In the 2013 compilation, there are 896 nuclei, which has the experimental data of charge radii. These nuclei are chosen as the entire set. The global deviations for the charge radii between the theoretical results and experimental data can be

represented as standard deviation  $\sigma_{\text{rms}}$ :

$$\sigma_{\text{rms}}^2 = \frac{1}{X} \sum_{x=1}^X [R_C^{\text{exp}}(x) - R_C^{\text{th}}(x)]^2. \quad (9)$$

#### 1. The NBP refinements for the HFB predictions

With the Skyrme-Hartree-Fock-Bogoliubov theories, we calculate the nuclear charge radii for the 896 nuclei in the entire set, and obtain the raw residuals  $\delta(Z, N)$  for each nucleus. In Table III, we present the standard deviation  $\sigma_{\text{pre}}$  of charge radii from the HFB model. The theoretical results from the HFB model are further refined by the NBP method.

For each target nucleus in the entire set, we select all the nuclei except the target nucleus as the sample set. The residuals of nuclei in the sample set are calibrated as a corresponding classification value  $\delta_i$  for a certain classification table. The prior probabilities  $P(Z)$ ,  $P(N)$ , and  $P(\delta_i)$  and the conditional probabilities  $P(Z|\delta_i)$ ,  $P(N|\delta_i)$  are calculated based on the classification table. With these probabilities, the posterior probabilities  $P(\delta_i|Z, N)$  for different classification values  $\delta_i$  are calculated by Eq. (7). The classification value  $\delta_i$  with the maximum posterior probability  $P(\delta_i|Z, N)$  is chosen as the estimated residual of the HFB model for the target nucleus. Following the same procedure, new estimated residuals for the target nucleus can be obtained, if different classification tables are used. During the calculations, 100 different classification tables are used for the prediction. Averaging all the results, the final predicted residual can be achieved. With the final

TABLE III. The standard deviations  $\sigma_{\text{pre}}(\text{fm})$  of  $R_C$  obtained from different nuclear charge radii models, and the standard deviations  $\sigma_{\text{post}}(\text{fm})$  after the NBP refinements. All the 896 nuclei with  $A > 3$  in the 2013 compilation [16] are chosen as the entire set.

Models	HFB	Sheng
$\sigma_{\text{pre}}$	0.0409	0.0287
$\sigma_{\text{post}}$	0.0239	0.0195
$\Delta\sigma/\sigma_{\text{pre}}$	41%	32%

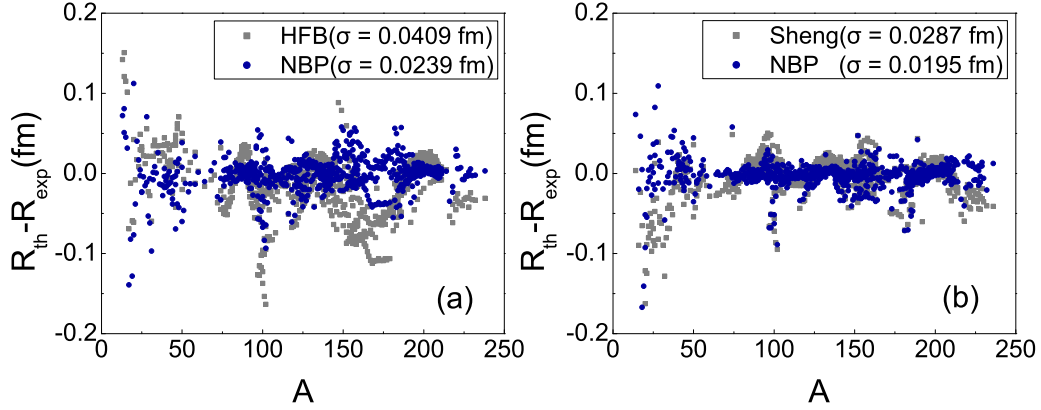


FIG. 1. (a) The charge radii residuals  $\delta(Z, N) = R_{\text{th}} - R_{\text{exp}}$  from the experimental data as a function of mass number  $A$ . The gray squares denote the raw results from the HFB calculations, and the blue dots denote the predicted residuals after the NBP refinements. (b) The same as (a), but for the results from Sheng's formula Eq. (10).

predicted residuals from the NBP method, the theoretical results of HFB model can be refined.

In Fig. 1(a), we show the refined results of all nuclei. The gray squares represent the raw residuals from the HFB model, and the blue dots represent the predicted residuals after the NBP refinements. From this figure one can see the accuracy of charge radii predictions has noticeable improvements by the NBP method, especially for the heavy nuclei. We calculate the  $\sigma_{\text{post}}$  of predicted  $R_C$  after the NBP refinements, and the results are presented in Table III. With the NBP method, the accuracy of charge radii predictions from the HFB model improves 41%.

## 2. The NBP refinements for the semiempirical formula predictions

The semiempirical formula is another common method to describe the nuclear charge radii [24,25]. In this paper, the semiempirical formula of Sheng *et al.* in Ref. [25]:

$$R_C = r_0 \left[ 1 - a \left( \frac{N-Z}{A} \right) + b \frac{1}{A} + c \frac{P}{A} \right] A^{1/3} \quad (10)$$

is selected to discuss the abilities of global optimizations of the NBP method, where  $r_0 = 1.2320$  fm,  $a = 0.1542$ ,  $b = 1.3768$ , and  $c = 0.4286$ . The Casten factor  $P$  is defined as  $N_n \times N_p / (N_n + N_p)$ , where  $N_n$  and  $N_p$  are the valence protons and valence neutrons, respectively [25]. The following magic numbers are used to calculate the Casten factor  $P$ :  $Z_M = 2, 6, 14, 28, 50, 82$ ;  $N_M = 2, 8, 14, 28, 50, 82, 126$  [50,51]. In Eq. (10), the theoretical  $R_C$  of 896 nuclei in the entire set are calculated, and the standard deviation  $\sigma_{\text{pre}}$  of charge radii from Sheng's formula is 0.0287 fm.

The NBP method is further applied to refine the results of Sheng's semiempirical formula. For each target nucleus in the entire set, the sample set is also selected as all the nuclei except itself. The residuals  $\delta(Z, N)$  from the semiempirical formula of 896 nuclei are calibrated as different classification values  $\delta_i$  for certain classification tables. With Eq. (7), we calculate the posterior probabilities  $P(\delta_i|Z, N)$  for the classification values  $\delta_i$  by the prior probabilities  $P(Z)$ ,  $P(N)$ ,  $P(\delta_i)$  and the conditional probabilities  $P(Z|\delta_i)$ ,  $P(N|\delta_i)$ . The estimated residuals are chosen as the classification values  $\delta_i$

with the maximum posterior probability. Averaging all the estimated residuals from different classification tables, the final predicted residuals and the refined  $R_C$  can be obtained. For Sheng's formula, the standard deviation of charge radii after the NBP refinements is  $\sigma_{\text{post}} = 0.0195$  fm, which is also presented in Table III. Comparing  $\sigma_{\text{pre}}$  and  $\sigma_{\text{post}}$  from Sheng's formula, the accuracy of charge radii predictions improves 32% by applying the NBP method.

In Fig. 1(b), we also present the refined results for Sheng's semiempirical formula. The gray squares represent the raw results from the Sheng's formula, and the blue dots represent the predicted residuals after the NBP refinements. Similar to Fig. 1(a), there are also improvements for the accuracy of charge radii predictions by applying the NBP method.

It should be mentioned that the NBP method cannot predict the charge radii for all the nuclei. When the prior probability  $P(Z)$  or  $P(N)$  is zero, the predicted residual cannot be given (i.e., the proton number  $Z$  or neutron number  $N$  of target nucleus is vacant in the sample set). There are 878 nuclei in the entire set. For the HFB model and Sheng's semiempirical formula, we obtain 711 and 769 predicted results of charge radii, respectively.

By applying to the raw results of charge radii from the microscopic structure model and semiempirical formula, the global optimizations of the NBP method have convincing improvements, which can be seen in Table III and Fig. 1. Although the NBP method is only a fine-tuning for the charge radii, it could correct the defects even if the raw residuals are large.

## B. Extrapolating ability of NBP method

Extrapolations are always riskier than global optimizations. The properties of global optimizations of the NBP method were discussed in the previous section. In this part, the suitability of the NBP method is further analyzed by the extrapolations to the unknown regions of the nuclear chart. To show the extrapolating abilities of the NBP method, the nuclei in the entire set are divided into the learning set and validation set. In the 2004 compilation [14], there are 892 nuclei with mass number  $A > 3$ , which have the experimental

TABLE IV. The standard deviations  $\sigma_{\text{pre}}$  (fm) of  $R_C$  obtained from different nuclear charge radii models, and the standard deviations  $\sigma_{\text{post}}$  (fm) after the NBP refinements. All the 896 nuclei with  $A > 3$  in the 2013 compilation [16] are chosen as the entire set, the 787 nuclei with mass number  $A > 3$  in the 2004 compilation [14] are chosen as the learning set, and the remnant 109 nuclei in the entire set are chosen as the validation set.

Models	Learning set		Validation set		Entire set	
	HFB	Sheng	HFB	Sheng	HFB	Sheng
$\sigma_{\text{pre}}$	0.0415	0.0294	0.0332	0.0244	0.0409	0.0287
$\sigma_{\text{post}}$	0.0240	0.0200	0.0251	0.0196	0.0239	0.0195
$\Delta\sigma/\sigma_{\text{pre}}$	42%	32%	24%	20%	41%	32%

data of charge radii. The 786 nuclei in the 2004 compilation are chosen as the learning set, and the remnant 106 nuclei in the entire set are chosen as the validation set. Some adjustments are made that the nuclei  $^{92}\text{Mo}$ ,  $^{94-97}\text{Mo}$  in the 2004 compilation are put into the validation set and the  $^{90}\text{Y}$  is put into the learning set.

### 1. Extrapolations based on the HFB results

The extrapolation property of the NBP method is first discussed based on the HFB results. With the HFB model, we calculate the standard deviations  $\sigma_{\text{pre}}$  for the learning set and validation set, and the results are presented in Table IV. For the learning set, the raw predictions from the HFB model generate  $\sigma_{\text{pre}} = 0.0415$  fm; for the validation set, the raw predictions from HFB model generate  $\sigma_{\text{pre}} = 0.0332$  fm. This means the HFB model has extrapolating ability, and is a global method to describe the nuclear charge radii. By applying the NBP method, the standard deviations of  $R_C$  for the learning set is  $\sigma_{\text{post}} = 0.0234$  fm, and the accuracy of charge radii predictions improves 42%.

With the raw residuals from the HFB model in the learning set, the residuals of charge radii in the validation set are predicted by the NBP method. In Table IV, we present the standard deviations for the predicted  $R_C$  of validation set  $\sigma_{\text{post}} = 0.0251$  fm, and the accuracy of charge radii predictions improves 24%. By comparing the  $\Delta\sigma/\sigma_{\text{pre}}$  of the learning set and the validation set, one can see the NBP method has good extrapolating ability, and can be used to predict the charge radii of unknown regions in the nuclear chart.

For the nuclei with raw residuals  $|\delta_{\text{raw}}| > 0.05$  fm in the validation set, their refined residuals  $|\delta_{\text{refi}}|$  are presented in Table V. The predicted charge radii  $R_C$  with error bars  $\Delta R_C^{\text{refi}}$  after the NBP refinement are also presented in this table to compared with the experimental data. One can see that there are significant improvements in the charge radii predictions after the NBP refinements. This is because of the local relations for nuclei with the same proton number  $Z$  or neutron number  $N$ . The HFB model is constructed by the mean field approximations, and the residual interactions of nucleons are not included in the model [27]. However, in the naive Bayesian formula Eq. (7), the inner relations of  $R_C$  for nuclei with the same  $Z$  or  $N$  are reflected by means of the

TABLE V. All nuclei in the validation set with the raw residuals  $|\delta_{\text{raw}}| > 0.05$  fm from the HFB model, and the corresponding refined residuals  $|\delta_{\text{refi}}|$  from the NBP method. The corresponding refined charge radii  $R_C$  together with the errors  $\Delta R_C^{\text{refi}}$  are also presented in this table.

$Z$	$N$	$ \delta_{\text{raw}} $	$ \delta_{\text{refi}} $	$R_C^{\text{expt}}$	$R_C^{\text{refi}}$	$\Delta R_C^{\text{refi}}$
38	39	0.050	0.020	4.257	4.277	0.004
42	60	0.066	0.023	4.491	4.468	0.018
42	62	0.079	0.053	4.525	4.472	0.008
42	66	0.074	0.037	4.561	4.524	0.015
52	64	0.051	0.050	4.709	4.659	0.003
70	99	0.064	0.006	5.277	5.283	0.005
70	105	0.060	0.010	5.313	5.323	0.004
72	99	0.062	0.008	5.304	5.312	0.004
84	132	0.053	0.035	5.636	5.601	0.002

statistical method. Therefore, the NBP method can be seen as the combination of local relations and global descriptions.

### 2. Extrapolations based on the semiempirical formula's results

The extrapolating ability of the NBP method is further tested with the results of the semiempirical formula. With Sheng's formula in Eq. (10), the standard deviations  $\sigma_{\text{pre}}$  of the learning set and validation set are also calculated to be 0.0294 fm and 0.0244 fm, respectively, and the results are shown in Table IV. By comparing the  $\sigma_{\text{pre}}$  of the learning set and the validation set from Sheng's formula, one can see that Sheng's semiempirical formula can provide global descriptions for the nuclear charge radii.

Based on the raw results of Sheng's formula in the learning set, the NBP method is further applied to predict the residuals of the validation set. The standard deviations for the predicted  $R_C$  of the validation set are presented in Table IV. The accuracy of the predicted charge radii in the validation set improves 20% after the NBP refinements. By comparing the  $\Delta\sigma/\sigma_{\text{pre}}$  of the learning set and the validation set, it can be seen that the NBP method has extrapolating ability, when applied to the results of the semiempirical formula.

From Tables IV and V, it can be concluded that the NBP method has good extrapolating abilities. Based on both the advantages of the local relations and global descriptions, the charge radii of unknown regions of the nuclear chart can be predicted by the NBP method. There are also inadequacies for the NBP extrapolations. For certain nuclei in the validation set, their charge radii cannot be refined by the NBP method, when the proton number  $Z$  or neutron number  $N$  is vacant in the learning set. There are 109 nuclei in the validation set. We obtain 71 refined charge radii for the HFB model, and 82 refined charge radii for the Sheng's semiempirical formula.

### C. The NBP refinements for the isotopes

The odd-even effect are common phenomena in many nuclear properties, and the phenomena can also be observed in nuclear charge radii and nuclear mass [25]. The interactions between the last proton and the last neutron of nuclei lead to the statistical odd-even features in nuclear properties [21].

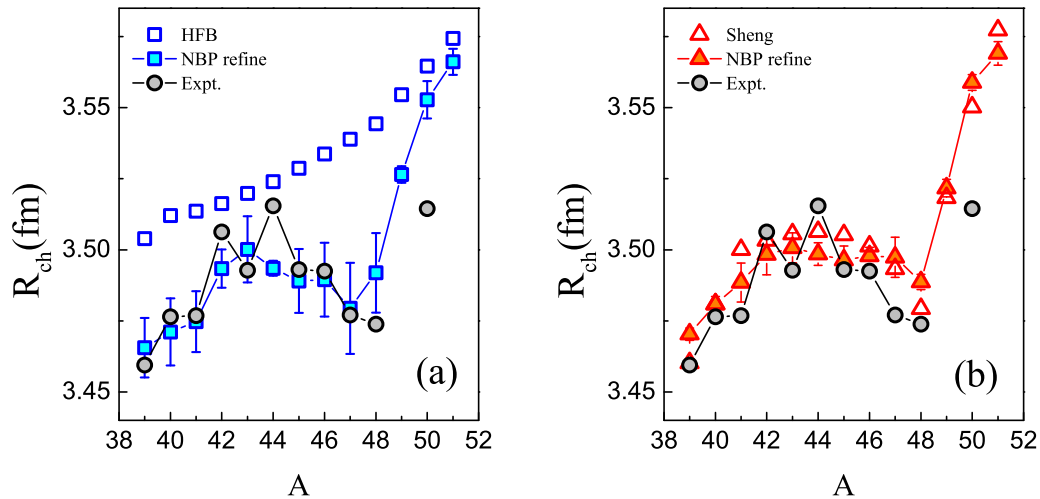


FIG. 2. (a) The theoretical and experimental charge radii  $R_C$  for Ca isotopes. Predictions are displayed without error bars for the raw results of the HFB model, and with error bars after the NBP refinements. (b) The same as (a), but for the predictions from Sheng's semiempirical formula.

After illustrating the global descriptions and extrapolating abilities of the NBP method, the refined charge radii of Ca and Bi isotopes are further displayed to reflect the predicting abilities of the NBP method for the odd-even staggering. The results of Ca isotopes are presented in Fig. 2, and reflect the cases of even-even and odd-A nuclei; the results of Bi isotopes are presented in Fig. 3 and reflect the cases of odd-A and odd-odd nuclei.

The studies on the trend of charge radii  $R_C$  of the Ca isotopic chain is a very interesting topic in nuclear physics, which can reflect many underlying physics in the nuclear structure [52]. The  $R_C$  of  $^{40}\text{Ca}$  and  $^{48}\text{Ca}$  are also most identical, and the odd-even effects are more evident for the Ca isotopes between  $N = 20$  to  $N = 28$  compared with other observables in the nuclear chart. For isotopes beyond  $N = 28$ , there is a noticeable increase in charge radii. However, the results

from the mean-field models fail to describe these properties of charge radii of Ca isotopes, which can be seen in Fig. 2 of this paper and Fig. 4 of Ref. [53]. Based on the results of the HFB model the refined  $R_C$  from the NBP method can well reproduce the changing feathers of Ca isotopes, which can be seen in Fig. 2(a). Not just the results from the HFB model, the refinements on the semiempirical formula are provided in Fig. 2(b), which also coincide with the experimental data. The results in Fig. 2 show that the effects of the pairing correlations and other nucleon-nucleon relations on charge radii of Ca isotopes can be reflected in the NBP method.

In addition to the Ca isotopes, the charge radii  $R_C$  of Bi isotopes from the HFB model and Sheng's semiempirical formula are presented in Fig. 3. The refined charge radii by the NBP method are also presented in these figures for comparison. In Fig. 3(a), one can see for the HFB model,

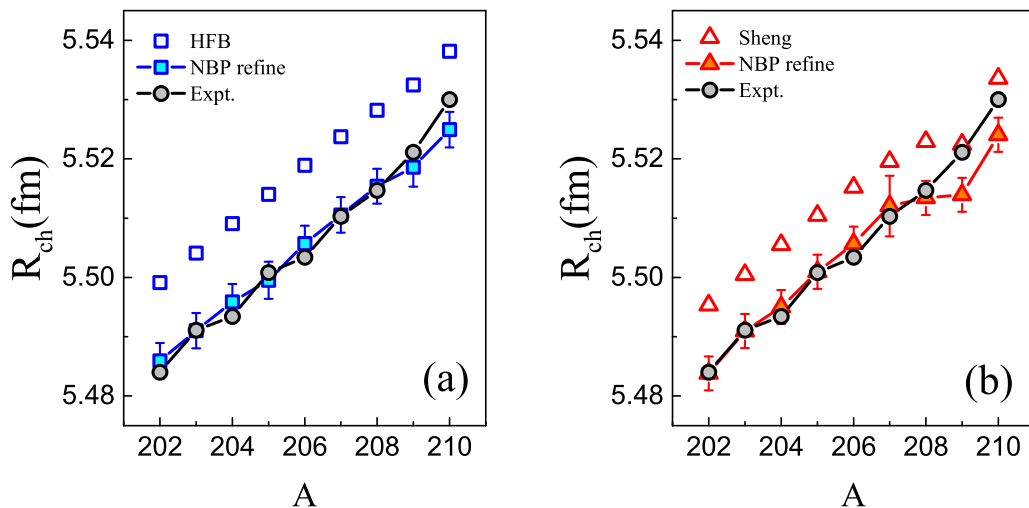


FIG. 3. (a) The theoretical and experimental charge radii  $R_C$  for Bi isotopes. Predictions are displayed without error bars for the raw results of the HFB model, and with error bars after the NBP refinements. (b) The same as (a), but for the predictions from Sheng's semiempirical formula.

the predicted accuracy of charge radii of the odd-A and odd-odd Bi isotopes have definite improvements after NBP refinements. Similar results are also displayed in Fig. 3(b) for Sheng's semiempirical formula, and the improvements for the predicted accuracy of charge radii are also impressive.

Figures 2 and 3 reflect the essence of the NBP method. The HFB model and the semiempirical formula can provide robust global descriptions on the nuclear charge radii, and these descriptions can be systematically improved by the NBP method. That is from the local correlations of nuclear properties for the nuclei with the same  $Z$  or  $N$ . The odd-even features of raw residuals in Figs. 2 and 3 reflect the interactions between the last proton and last neutron in nuclei, which are neglected in the HFB model and Sheng's formula. From the Bayesian formula, these odd-even features can be considered by the statistical approach, which lead to reasonable results in  $R_C$  descriptions. The charge radii predictions in Figs. 2 and 3 have satisfactory improvements, and show the abilities of the NBP method for the odd-even staggering. Therefore, the unknown charge radii of isotopes can be predicted by the NBP method.

#### IV. SUMMARY

The nuclear charge radii are an important quantity to study the nuclear structure. There are many methods to describe the nuclear charge radii, such as the microscopic nuclear structure models and the semiempirical formulas. In the last few years, many pioneering studies are carried out to analyze the nuclear properties based on the Bayesian neural network method. To better study the data structure and analyze the inner numerical relationships, a developed method is proposed in this paper by combining the nuclear structure models with the naive Bayesian probability (NBP) classifier.

Several sets are chosen to test the reliabilities of the NBP method, which are the entire set (896 nuclei in the 2013 compilation), the learning set (787 nuclei in the 2004 compilation), and the validation set (109 nuclei calibrated from 2004 to 2013). The properties of global optimizations for the NBP method are discussed first. For the entire set, the standard deviations are presented in Table III. The accuracy of charge radii descriptions improves 41% and 32% for the HFB and Sheng's semiempirical formula, respectively. Secondly, the extrapolating abilities of the NBP method are analyzed. The

standard deviations  $\sigma_{\text{pre}}$  of the learning set and validation set are presented in Table IV, which are calculated from the raw results of the HFB model and Sheng's formula. With the NBP method, the charge radii for the validation set are predicted by the raw residuals of the learning set, and the corresponding  $\sigma_{\text{post}}$  are also presented in Table IV. One can see that the NBP method has reliable extrapolating abilities by comparing the  $\Delta\sigma/\sigma_{\text{pre}}$  of the learning set and validation set. Finally, we analyze the predicting abilities of the NBP method for the isotopic chains. The changing feathers of the charge radii for Ca and Bi isotopes can be well reproduced by the NBP method.

The accuracy of charge radii predictions has impressive improvements with the application of the NBP method, which is because of the statistical relationship in the NBP method. The nuclear model can fully describe the main changing trends of charge radii, and the NBP method can offer necessary fine-tuning. Based on the global descriptions, the local statistical association of the nuclear properties with the same proton number  $Z$  or neutron number  $N$  are taken into account statistically in the framework of the NBP method. Combining the global descriptions with the local correlations, the NBP method shows reliable capacities in predicting the nuclear charge radii for both the interpolation and extrapolation. It should be noted that there are limitations for applying the NBP method. Because the predictions are directly connected with the experimental data, the  $R_C$  of certain nuclei cannot be estimated if the corresponding prior probabilities and conditional probabilities are missing in the data sets. In the case of interpolation, 769 results are obtained for 878 candidates, and in the case of extrapolation, 82 results are obtained for 109 candidates. The NBP method developed in this paper can also be used to study other nuclear properties, such as nuclear mass, nuclear decay, and nuclear reactions.

#### ACKNOWLEDGMENTS

The authors are grateful to Pawel Danielewicz for valuable discussions and careful reading of the paper. This work is supported by the National Natural Science Foundation of China (Grants No. 11505292, No. 11535004, No. 11822503, No. 11575082, and No. 11605105), by the Fundamental Research Funds for the Central Universities (Grants No. 17CX02044 and No. 15CX07005A), and by the China Scholarship Council (CSC).

- 
- [1] A. Bohr, B. R. Mottelson, and G. Breit, *Phys. Today* **23**(9), 58 (1970).
  - [2] I. Angeli, Y. P. Gangrsky, K. Marinova, I. Boboshin, S. Y. Komarov, B. Ishkhanov, and V. Varlamov, *J. Phys. G* **36**, 085102 (2009).
  - [3] B. G. Todd-Rutel and J. Piekarewicz, *Phys. Rev. Lett.* **95**, 122501 (2005).
  - [4] W.-C. Chen and J. Piekarewicz, *Phys. Rev. C* **90**, 044305 (2014).
  - [5] J. Liu, X. Zhang, C. Xu, and Z. Ren, *Nucl. Phys. A* **948**, 46 (2016).
  - [6] J. Liu, R. Xu, J. Zhang, C. Xu, and Z. Ren, *J. Phys. G* **46**, 055105 (2019).
  - [7] P.-C. Chu, Y. Zhou, X. Qi, X.-H. Li, Z. Zhang, and Y. Zhou, *Phys. Rev. C* **99**, 035802 (2019).
  - [8] M. Avgoulea *et al.*, *J. Phys. G* **38**, 025104 (2011).
  - [9] A. Krieger, K. Blaum, M. L. Bissell, N. Frommgen, C. Geppert, M. Hammen, K. Kreim, M. Kowalska, J. Kramer *et al.*, *Phys. Rev. Lett.* **108**, 142501 (2012).
  - [10] D. Ni, Z. Ren, T. Dong, and Y. Qian, *Phys. Rev. C* **87**, 024310 (2013).
  - [11] M. Bazzi *et al.*, *Phys. Lett. B* **697**, 199 (2011).



- [12] G. Ewald, W. Nortershauser, A. Dax, S. Gotte, R. Kirchner, H.-J. Kluge, Th. Kuhl, R. Sanchez, A. Wojtaszek, B. A. Bushaw, G. W. F. Drake, Z.-C. Yan, and C. Zimmermann, *Phys. Rev. Lett.* **93**, 113002 (2004).
- [13] S. Zhang, J. Meng, S.-G. Zhou, and J. Zeng, *Eur. Phys. J. A* **13**, 285 (2002).
- [14] I. Angeli, *At. Data Nucl. Data Tables* **87**, 185 (2004).
- [15] R. G. Arnold, C. E. Carlson, and F. Gross, *Phys. Rev. C* **21**, 1426 (1980).
- [16] I. Angeli and K. P. Marinova, *At. Data Nucl. Data Tables* **99**, 69 (2013).
- [17] J. Piekarewicz, M. Centelles, X. Roca-Maza, and X. Vinas, *Eur. Phys. J. A* **46**, 379 (2010).
- [18] B. H. Sun, Y. Lu, J. P. Peng, C. Y. Liu, and Y. M. Zhao, *Phys. Rev. C* **90**, 054318 (2014).
- [19] M. Bao, Y. Lu, Y. M. Zhao, and A. Arima, *Phys. Rev. C* **94**, 064315 (2016).
- [20] M. Liu, N. Wang, Y. Deng, and X. Wu, *Phys. Rev. C* **84**, 014333 (2011).
- [21] Y. Y. Cheng, Y. M. Zhao, and A. Arima, *Phys. Rev. C* **89**, 061304(R) (2014).
- [22] K. Pomorski and J. Dudek, *Phys. Rev. C* **67**, 044316 (2003).
- [23] G. Royer and R. Rousseau, *Eur. Phys. J. A* **42**, 541 (2009).
- [24] N. Wang and T. Li, *Phys. Rev. C* **88**, 011301(R) (2013).
- [25] Z. Sheng, G. Fan, J. Qian, and J. Hu, *Eur. Phys. J. A* **51**, 40 (2015).
- [26] D. Vautherin and D. M. Brink, *Phys. Rev. C* **5**, 626 (1972).
- [27] P.-G. Reinhard, *Rep. Prog. Phys.* **52**, 439 (1989).
- [28] M. Bender, P. H. Heenen, and P. G. Reinhard, *Rev. Mod. Phys.* **75**, 121 (1996).
- [29] L. S. Geng, H. Toki, S. Sugimoto, and J. Meng, *Prog. Theor. Phys.* **110**, 921 (2003).
- [30] M. V. Stoitsov, J. Dobaczewski, W. Nazarewicz, S. Pittel, and D. J. Dean, *Phys. Rev. C* **68**, 054312 (2003).
- [31] J. Liu, C. Xu, and Z. Ren, *Phys. Rev. C* **95**, 044318 (2017).
- [32] T. Liang, J. Liu, Z. Ren, C. Xu, and S. Wang, *Phys. Rev. C* **98**, 044310 (2018).
- [33] R. Utama, J. Piekarewicz, and H. B. Prosper, *Phys. Rev. C* **93**, 014311 (2016).
- [34] R. Utama, W.-C. Chen, and J. Piekarewicz, *J. Phys. G* **43**, 114002 (2016).
- [35] L. Neufcourt, Y. Cao, W. Nazarewicz, and F. Viens, *Phys. Rev. C* **98**, 034318 (2018).
- [36] L. Neufcourt, Y. Cao, W. Nazarewicz, E. Olsen, and F. Viens, *Phys. Rev. Lett.* **122**, 062502 (2019).
- [37] R. Utama and J. Piekarewicz, *Phys. Rev. C* **97**, 014306 (2018).
- [38] Y. He, L.-G. Pang, and X.-N. Wang, *Phys. Rev. Lett.* **122**, 252302 (2019).
- [39] Z. M. Niu, H. Z. Liang, B. H. Sun, W. H. Long, and Y. F. Niu, *Phys. Rev. C* **99**, 064307 (2019).
- [40] G. A. Negoita *et al.*, *Phys. Rev. C* **99**, 054308 (2019).
- [41] J. A. Benediktsson, P. H. Swain, and O. K. Ersoy, *IEEE Transactions on Geoscience and Remote Sensing* **28**, 540 (1990).
- [42] J. V. Tu, *J. Clin. Epidemiol.* **49**, 1225 (1996).
- [43] K. M. Graczyk and C. Juszczak, *Phys. Rev. C* **90**, 054334 (2014).
- [44] K. M. Graczyk, *Phys. Rev. C* **88**, 065205 (2013).
- [45] R. M. Neal, *Bayesian Learning for Neural Networks* (Springer Science & Business Media, Berlin/Heidelberg, 2012).
- [46] T. H. R. Skyrme, *Nucl. Phys.* **9**, 615 (1958).
- [47] N. Wang, M. Liu, H. Jiang, J. L. Tian, and Y. M. Zhao, *Phys. Rev. C* **91**, 044308 (2015).
- [48] J. Liu, C. Xu, S. Wang, and Z. Ren, *Phys. Rev. C* **96**, 034314 (2017).
- [49] D. R. Bellhouse, *Stat. Sci.* **19**, 3 (2004).
- [50] R. F. Casten, D. S. Brenner, and P. E. Haustein, *Phys. Rev. Lett.* **58**, 658 (1987).
- [51] I. Angeli, *J. Phys. G* **17**, 439 (1991).
- [52] R. F. Garcia Ruiz, *Nat. Phys.* **12**, 594 (2016).
- [53] Z. Wang and Z. Ren, *Phys. Rev. C* **71**, 054323 (2005).